Artificial Organs

WILEY

Artificial Organs

MAIN TEXT OPEN ACCESS

Physiological Control of Realheart Total Artificial Heart

Emanuele Perra[1] | Daniel Jonasson[2] | Shaikh Faisal Zaman[2] | Nils Brynedal Ignell[2] | Michael Broomé[3,4] | Thomas Finocchiaro[2] | Ina Laura Perkins[2] | Seraina Anne Dual[1]

[1]Intelligent Heart Technology Lab, Department of Biomedical Engineering and Health Systems, KTH Royal Institute of Technology, Stockholm, Sweden | [2]Scandinavian Real Heart AB, Västerås, Sweden | [3]Anesthesia and Intensive Care, Department of Physiology and Pharmacology, Karolinska Institute, Stockholm, Sweden | [4]ECMO Department, Karolinska University Hospital, Stockholm, Sweden

Correspondence: Seraina Anne Dual (seraina.dual@alumni.ethz.ch)

Received: 10 January 2025 | **Revised:** 11 May 2025 | **Accepted:** 27 May 2025

Funding: The work was carried out within the strategic innovation programme 'Smarter Electronics Systems', a joint initiative by Vinnova, Formas and the Swedish Energy Agency (Energimyndigheten). VINNOVA : 2022-00849; 2024-00592. Digital Futures.

Keywords: cardiovascular system modeling | hybrid mock loop | physiological control | pulmonary hypertension | total artificial heart

ABSTRACT

Background: Heart failure (HF) affects approximately 64 million patients worldwide, where the heart's impaired ability to pump blood leads to reduced quality of life and a high 5-year mortality rate. Total artificial hearts (TAHs) offer a promising solution, but to ensure a good quality of life and prolong life expectancy for end-stage HF patients, TAHs must adapt to the body's varying metabolic demands.

Methods: This study evaluates the physiological control performance of the Realheart TAH using a hybrid mock circulation loop that simulates dynamic physiological states, such as sleep, rest, and exercise. The Realheart TAH features a preload-based control mechanism that adjusts heart rate (HR) and stroke volume (SV) in response to changes in atrial pressure, closely mimicking the native heart's ability to meet varying blood flow demands. The controller's adaptability and robustness were further tested under different levels of pulmonary vascular resistance (PVR), simulating conditions that challenge flow balance.

Results: The results demonstrate that the Realheart TAH maintains flow balance between the right and left ventricles and stabilizes atrial pressures across all tested conditions. During simulated exercise, the controller increased cardiac output (CO) by up to 2.1 times from rest while maintaining stable atrial pressures, compared to a maximum increase of 1.2 times without the controller. During sleep, CO decreased by 25%, whereas a decrease of only 5% was observed without the controller. Under increased PVR, the controller adjusted SV and HR to preserve consistent CO and prevent blood volume build-up in the atria, which could otherwise lead to dangerously high atrial pressures.

Conclusion: The physiological control system demonstrated its ability to adapt to rapid transitions between physiological states, although occasional undershoots in pressure were observed during transitions from exercise to rest conditions. This study highlights the Realheart TAH's ability to autonomously adjust to varying physiological conditions and patient needs, showing promise for treating patients with advanced HF. Future work will focus on optimizing the control system to further enhance the device's responsiveness and stability during rapid physiological transitions.

Abbreviations: CO, cardiac output; HF, heart failure; HMCL, hybrid mock circulation loop; HR, heart rate; LAP, left atrial pressure; PH, pulmonary hypertension; PVR, pulmonary vascular resistance; RAP, right atrial pressure; SL, stroke length; SV, stroke volume; SVR, systemic vascular resistance; TAH, total artificial heart; UVV, unstressed venous volume; VAD, ventricular assist device.

1 | Introduction

Heart failure (HF) affects about 64 million patients globally and is characterized by impaired cardiac output (CO) and filling pressures, resulting in poor quality of life [1] and a 5-year mortality rate of 45%–60% [2, 3]. Heart transplantation remains the gold standard for advanced HF but is hindered by limited donor availability and stringent eligibility criteria. Elevated pulmonary hypertension (PH), defined as a mean pulmonary arterial pressure (mPAP) > 20 mmHg at rest [4], is a common contraindication, as it exposes the donor heart's right ventricle to high afterload, risking acute right HF. Up to 60% of advanced HF patients develop PH, leaving them with few therapeutic options [5, 6].

Total artificial hearts (TAHs) have emerged as potential solutions for end-stage HF, offering either temporary or permanent mechanical circulatory support. While active physiological adaptation remains a long-standing goal in TAH development, which is essential for meeting varying perfusion demands, it is not yet a standard feature in current systems. In the related field of ventricular assist devices (VADs), research indicates that preload-dependent physiological control is necessary to dynamically support the heart in response to the body's changing metabolic needs during different activities [7–9]. Yet, traditional VADs still operate with fixed parameters, limiting their adaptability to varying patient needs [10, 11]. In contrast, newer pre-clinical TAHs are being designed to enable preload-responsive control, aiming to mimic the Frank-Starling mechanism to improve flow regulation [12–14].

The SynCardia TAH, one of the few FDA-approved devices, uses pneumatically driven ventricles and relies on passive preload-dependent filling to regulate flow [15]. However, its lack of active control can lead to imbalances in right and left output, particularly in patients with PH, where issues such as significant pulmonary edema have been reported [16].

Next-generation TAHs aim to address these limitations. BiVACOR's compact continuous-flow TAH employs magnetically levitated impellers, passive flow balancing, and speed modulation without blood-contact sensors. Although pulsatile flow is achieved through cyclic speed changes, it does not replicate true native pulsatility [17]. Similarly, Carmat SA's Aeson TAH uses an electrohydraulic system with bioprosthetic valves and pulsatile flow, actively adjusting stroke volume (SV) and heart rate (HR) to prevent inflow pressure imbalance. However, its large size limits use to select patients [13].

Despite these advances, key challenges remain, including device miniaturization, ease of implantation, and enhanced adaptability for broader patient use. While SynCardia paved the way for clinical application, ongoing efforts aim to address unmet clinical needs.

The Realheart TAH (Scandinavian Real Heart AB, Sweden) offers a physiologically pulsatile solution driven by two electric motors, featuring atrial pressure sensors and active control to dynamically adjust HR and SV based on preload [18]. This mimics the Frank-Starling law, where increased venous return leads to increased SV and CO [19].

In this study, we evaluated Realheart's physiological controller performance using a hybrid mock circulation loop (HMCL) under simulated dynamic conditions (i.e., sleep, rest, exercise). This benchtop method replicates physiological scenarios through in vitro and in silico modeling. Our findings demonstrate Realheart's performance in maintaining balanced right/left ventricular flow under varying afterload and preload, highlighting the advantages and limitations of active preload-based control in TAHs.

2 | Methods

2.1 | The Realheart Total Artificial Heart

The Realheart TAH is a four-chamber device designed to mimic the human heart, consisting of two pumps, each containing an atrium and a ventricle. Each pump is driven by an electric motor, with the atria and ventricles separated by an atrio-ventricular (AV) plane, which houses the mitral and tricuspid valves. Valves at the outflows simulate the aortic and pulmonary valves (Figure 1a). During systole, the mitral valve closes as the piston moves downward, ejecting blood through the aortic valve. During diastole, the piston retracts, the mitral valve opens, and the aortic valve closes, allowing ventricular filling.

The flow on each side can be independently adjusted by modifying the stroke length (SL) and operating frequency, which is synchronized between the two units. The AV plane, actuated by a brushless DC motor through a rack-and-pinion system, regulates ventricular pressure and blood flow. SL, determining the blood volume per cycle, is mechanically controlled. In this study, Version 11.4 of Realheart is used for the experiments.

2.2 | The Physiological Controller

The Realheart's active physiological feedback controller uses a preload-dependent mechanism based on the Frank-Starling law. Left and right atrial pressures (LAP and RAP, respectively) are used as feedback parameters, as they reflect cardiac preload, and are crucial for maintaining flow balance between the pumps [20–22].

The system adjusts SV and HR to maintain atrial pressures at predefined set points, adjustable by medical professionals. In this study, these are set to 9 and 4 mmHg for the left and right atrium, respectively. Two proportional-integral (PI) controllers manage the pressure difference and output the desired CO to keep pressures stable (Figure 1b). The controllers synchronize HR and independently modulate SVs for each pump unit.

The pump modulates pumping settings to achieve the target CO, initially adjusting HR bpm and then modulating SLs as HR elevates. The algorithm prioritizes keeping HR under 140 bpm by maximizing SL. In cases where both SL and HR reach their operational limits without satisfying the CO demand, the pump can switch to an extreme mode, allowing HR to increase up to 155 bpm, which is the safety HR threshold.

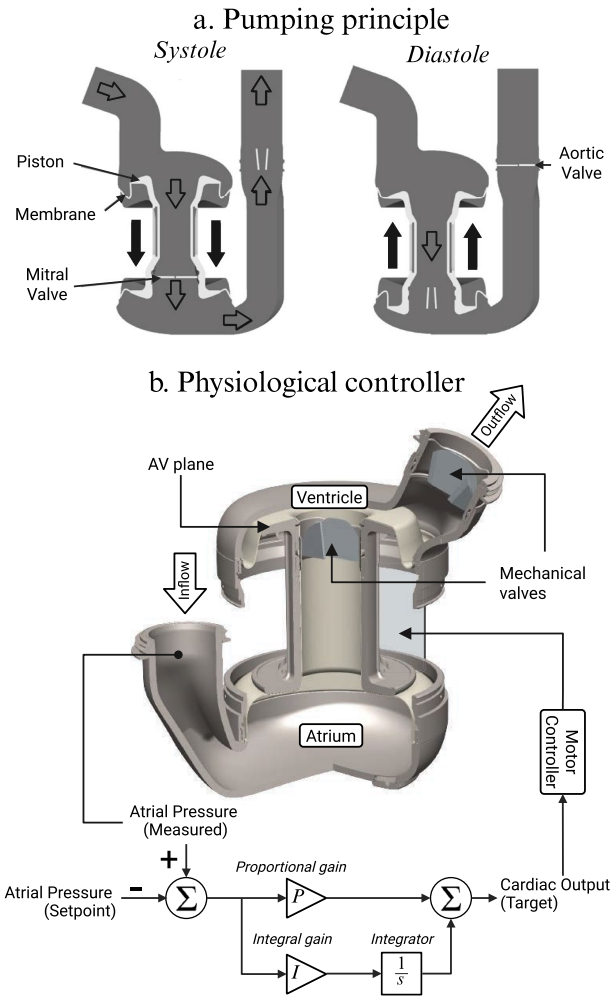

FIGURE 1 | (a) Pumping principle of the Realheart total artificial heart (TAH). The device uses a piston-driven system to replicate the cardiac cycle. During systole, the mitral valve closes as the piston moves downward, ejecting blood through the aortic valve. During diastole, the piston retracts, the mitral valve opens, and the aortic valve closes, allowing ventricular filling. (b) An external motor controller drives the motor, ejecting the blood through the outflow port, while a physiological controller regulates motor operation based on atrial pressure, enabling real-time adjustment of heart rate and stroke volume to mimic natural cardiac function and meet varying physiological demands. [Color figure can be viewed at wileyonlinelibrary.com] [Color figure can be viewed at wileyonlinelibrary.com]

2.3 | Hybrid Mock Circulation Loop

The HMCL system used in this study is adapted from previous models developed at ETH Zurich [23–25]. While no additional validation was performed using a conventional mock loop for this specific study, consistency was confirmed by comparing our results to those of prior Realheart studies conducted under comparable static and dynamic conditions [26].

The HMCL system consists of four fluid reservoirs (R1, R2, R3, R4) where fluid pressure is controlled by modulating the pressure in the air cavities of hermetically sealed reservoirs. Air valves (PVQ33-5G-23-01F and PVQ33-5G-40-01F; SMC Pneumatics, Tokyo, Japan) manage the pressurized air exchange, while pressure sensors (PN2099; IFM Electronic Geräte GmbH & Co. KG, Essen, Germany) monitor fluid pressure. Backflow pumps (RP1 and RP2; Jabsco Pump 23 680–4103, Xylem Inc., Washington, USA) generate unidirectional flow, regulated by a feedforward controller based on real-time fluid flow measurements (sample frequency = 2000 Hz) using flow sensors (Sonoflow CO.55/190; Sonotec GmbH, Halle, Germany) and a PID controller adjusting pump speed based on fluid levels detected by infrared distance sensors (GP2Y0A51SK0F; Sharp K.K., Sakai, Japan). The fluid mixture consists of a water and glycerol solution (5:3 ratio), which simulates the viscosity of blood containing 40% hematocrit [27].

In this study, the Realheart is integrated into the HMCL for dynamic in-vitro experiments (Figure 2). The right unit is connected between R1 and R2 (right atrial and pulmonary artery pressures), and the left unit between R3 and R4 (left atrial and aortic pressures). Pressure waveforms applied to each reservoir are derived from a real-time numerical simulation of a virtual patient's cardiovascular system, which responds physiologically to the flow generated by the Realheart. The cardiovascular model and control algorithms were implemented in MATLAB Simulink and run as a real-time system via MicroLabBox (MicroLabBox, dSPACE GmbH, Paderborn, Germany) at 2000 Hz.

2.4 | Cardiovascular Model

A lumped-parameter model of the cardiovascular system was integrated into the HMCL for real-time interaction with the TAH. The cardiovascular model used in this study (Figure 3) is adapted from Broomé et al. [28]. The model utilizes 25 vascular compartments that represent various segments of the systemic and pulmonary circulations. Each vascular segment is modeled via a 4-element Windkessel model, employing physical dimensions and mechanical properties to derive the electrical analogy impedance. Simulations incorporating a healthy heart model were also conducted to compare the cardiac response of a native heart with that of the TAH during simulated sleep, rest, and exercise. The numerical model of the heart consists of 4 separate chambers, with their active and passive characteristics described by a "double Hill equation" approximating the cardiac time varying elastance [29]. Cardiac valves opening and closing dynamics were implemented according to Mynard et al. [30]. Additionally, pericardial and atrial as well as ventricular septal left–right heart interactions were considered in the model.

2.5 | Bench-Top Experiments

2.5.1 | Static Test

Static experiments using the HMCL evaluated the TAH's hemodynamic performance under fixed afterload and preload, comparing results with a previous pump model [26]. A stepwise pressure ramp was applied to each TAH unit while measuring output flow. For the left unit, the inlet pressure was fixed at 10 mmHg, and outlet pressure increased from 30 to 130 mmHg in 20 mmHg steps. Then, with outlet pressure at 100 mmHg, inlet pressure varied from 0 to 25 mmHg in 5 mmHg increments. The right unit was tested similarly: inlet pressure fixed

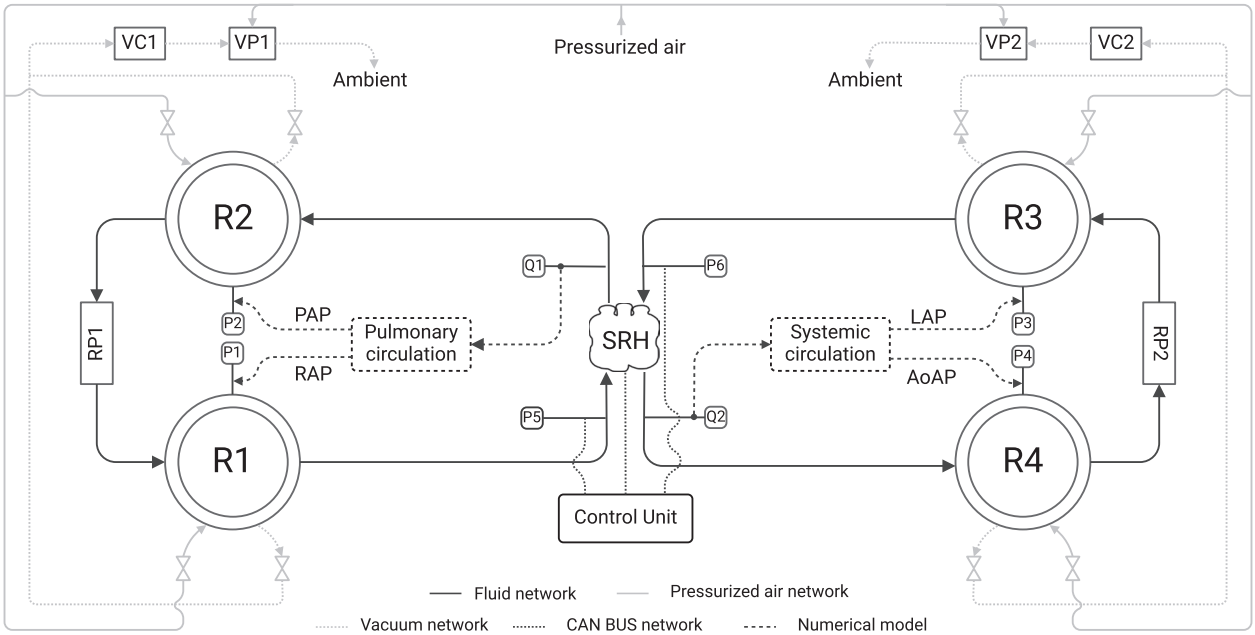

FIGURE 2 | Schematic of the hybrid mock circulation loop (HMCL) for evaluating the Scandinavian Realheart (SRH) TAH performance. The system simulates physiological conditions using integrated fluid, vacuum (VC1, VP1, VC2, VP2), and pressurized air networks. Four pressure-controlled fluid reservoirs (R1–R4) are used to model pulmonary and systemic circulation, with sensors measuring pressures (RAP, PAP, LAP, AoAP) and flow rates (Q1, Q2) generated by TAH. A control unit, linked via CAN BUS, dynamically adjusts pumping parameters in real time, enabling performance evaluation of the Realheart physiological controller under various physiological scenarios.

at 10 mmHg, outlet pressure increased from 15 to 45 mmHg in 5 mmHg steps, then outlet pressure held at 35 mmHg while varying inlet pressure from 0 to 20 mmHg. Each step lasted 10 s to reach steady state. Tests were performed at HRs of 60, 90, and 120 bpm with SLs of 19, 23, and 28 mm for the left unit (35, 45, and 55 mL) and 13, 18, and 22 mm for the right unit (20, 30, and 40 mL).

2.5.2 | Varying Pulmonary Hypertension Levels

This test evaluated the pump's performance (with physiological control on and off) under varying pulmonary vascular resistance (PVR). PVR values of 0.1, 0.2, 0.35, and 0.5 mmHg·s/mL were set by adjusting pulmonary resistance arterioli diameters, yielding mPAP levels of 15, 25, 40, and 50 mmHg, corresponding to healthy, mild, moderate, and severe PH conditions [31–33]. The Realheart pump, when operated with physiological control on and connected to the cardiovascular model via the HMCL, was tested under each PH condition. Each test was run for 100 s in triplicate. When operated without the physiological control, pumping parameters (HR, left SL, and right SL) were randomly varied within ±10% of the optimal values determined by the physiological controller at PVR = 0.1 mmHg·s/mL, to simulate operator error. These values were then held constant throughout the experiment.

2.5.3 | Induced Exercise State

Exercise was simulated by reducing SVR and PVR by 50% from baseline (SVR = 1 mmHg·s/mL; PVR = 0.1, 0.2, 0.35, 0.5 mmHg·s/mL) and lowering unstressed venous volume (UVV) by 500 mL, while keeping total blood volume constant, to increase cardiac filling. Each experiment lasted 250 s: 50 s at rest, 100 s during exercise, and 100 s at rest. Transitions between states were performed over 10 s to mimic an aggressive shift, as described by Petrou et al. [8], simulating worst-case conditions. The pump was tested with and without physiological control across PH levels, with each group tested in triplicate. Without control, pump parameters (HR, left SL, right SL) were randomly varied within ±10% of optimal values to simulate operator error, and held constant throughout the experiment

2.5.4 | Induced Sleep State

The sleep condition was modeled by increasing the SVR by 40% and keeping the PVR at its baseline. The UVV was increased by 300 mL to simulate the decreased metabolic demand during sleep [8]. Similarly to the exercise condition experiment, the experimental protocol consisted of running the pump for 50 s at rest, 100 s at sleep, and another 100 s at rest, with and without physiological control.

3 | Results

3.1 | Static Test

The results of the static tests are shown in Figures 4 and 5. The left pump's CO increases with SL and HR, ranging from 1.9 L/min to 9.6 L/min (Figure 4). At 60 bpm and a SL of 19 mm, CO reaches 2.8 L/min, decreasing to 1.9 L/min as afterload increases from 30 to 130 mmHg, with a fixed preload of 10 mmHg.

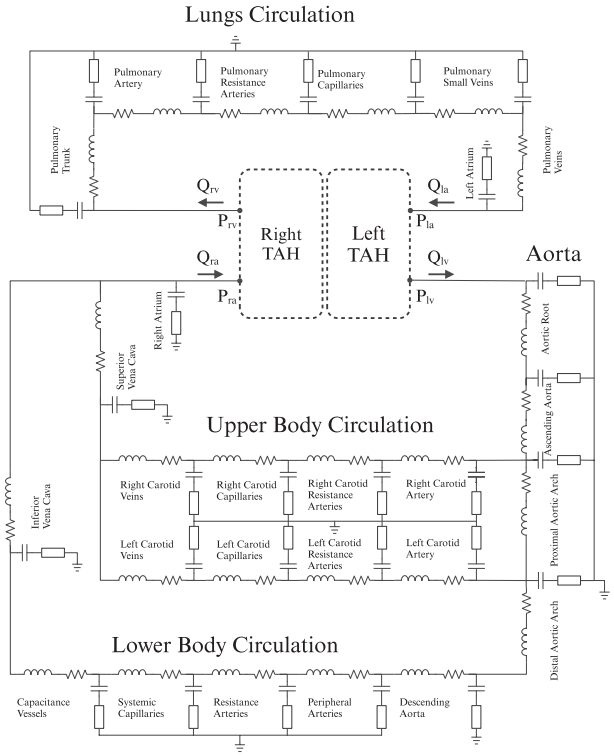

FIGURE 3 | This diagram shows the lumped-parameter model of the cardiovascular system used for hybrid testing of the TAH. The model includes components representing the systemic and pulmonary circulations, such as the aorta, carotid arteries, capillaries, vena cava, pulmonary arteries, and veins. It generates boundary conditions for TAH testing by providing right atrial pressure, pulmonary arterial pressure, left atrial pressure, and aortic pressure. These pressure waveforms are used to subject the TAH to different physiological scenarios.

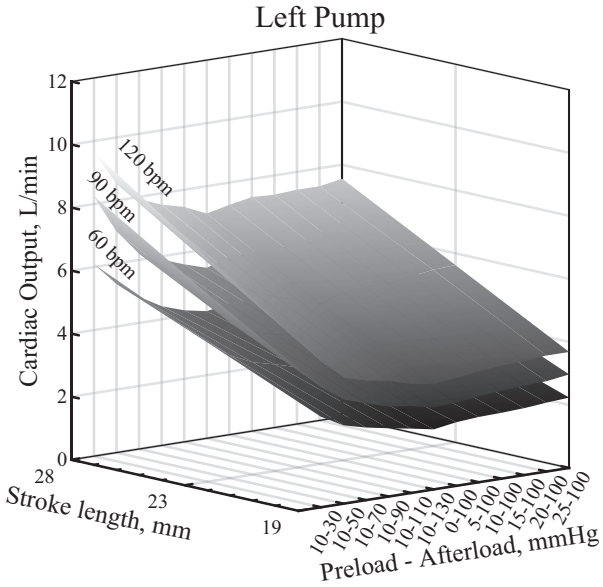

FIGURE 4 | Cardiac output of the left unit of the Realheart pump at different stroke lengts (19, 23 and 28 mm), heart rates (60, 90, 120 bpm) and different combinations of preload and afterload conditions.

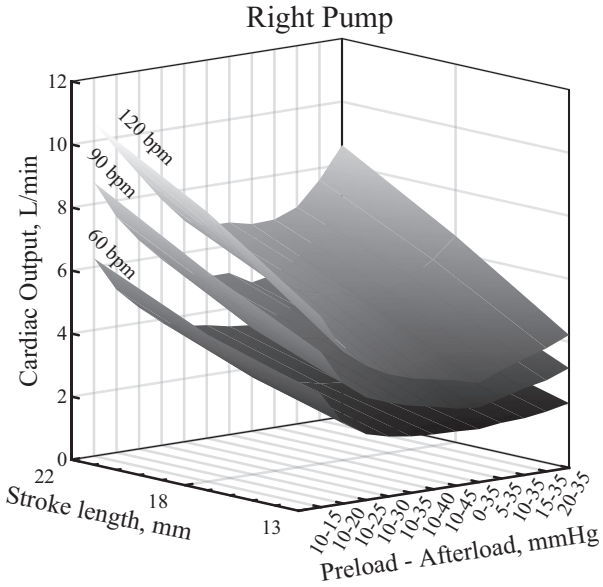

FIGURE 5 | Cardiac output of the right unit of the Realheart pump at different stroke lengths (13, 18 and 22 mm), heart rates (60, 90, 120 bpm) and different combinations of preload and afterload conditions.

Increasing preload from 0 mmHg to 25 mmHg slightly raises CO to 2.1 L/min at 100 mmHg afterload. The highest recorded CO is 9.6 L/min at 120 bpm and 28 mm SL.

The right pump exhibits a similar pattern, with CO ranging from 1.7 L/min to 10.6 L/min (Figure 5). At 60 bpm, CO is 3.6 L/min with 15 mmHg afterload and 10 mmHg preload, increasing to 6.3 L/min at a SL of 22 mm. At 120 bpm, CO reaches 6 L/min at the shortest SL and 10.6 L/min at the longest SL.

3.2 | Effect of Varying Pulmonary Hypertension on TAH Performance

Figure 6 shows results of the Realheart TAH tested with the physiological controller under different PVR levels, simulating various stages of PH.

As PVR increases, the physiological controller adjusts HR and SL: HR rises from 124.3 ± 1.1 bpm to 140.0 ± 0.0 bpm, while right and left SLs increase from 13.0 ± 0.1 mm to 16.6 ± 0.1 mm and from 16.6 ± 0.1 mm to 17.6 ± 0.3 mm, respectively. With control on, atrial pressures remain stable at 4 mmHg (right) and 9 mmHg (left). Without control, RAP rises with PVR from 3.6 ± 0.2 mmHg to 6.9 ± 0.8 mmHg, while LAP shows wide variability.

mPAP and MAP increase with PVR, reflecting hypertension behavior. CO rises with control on, from 4.1 ± 0.1 L/min to 4.9 ± 0.2 L/min (right) and from 4.2 ± 0.1 L/min to 5.1 ± 0.1 L/min (left), but decreases without control (Figure 6).

3.3 | TAH Response to Simulated Exercise Condition

During exercise, the physiological controller increases CO by 1.8–2.1 × the resting level across all PH levels, dynamically adjusting HR and SL (Figure 7). HR rises from 121.3 ± 0.6 bpm

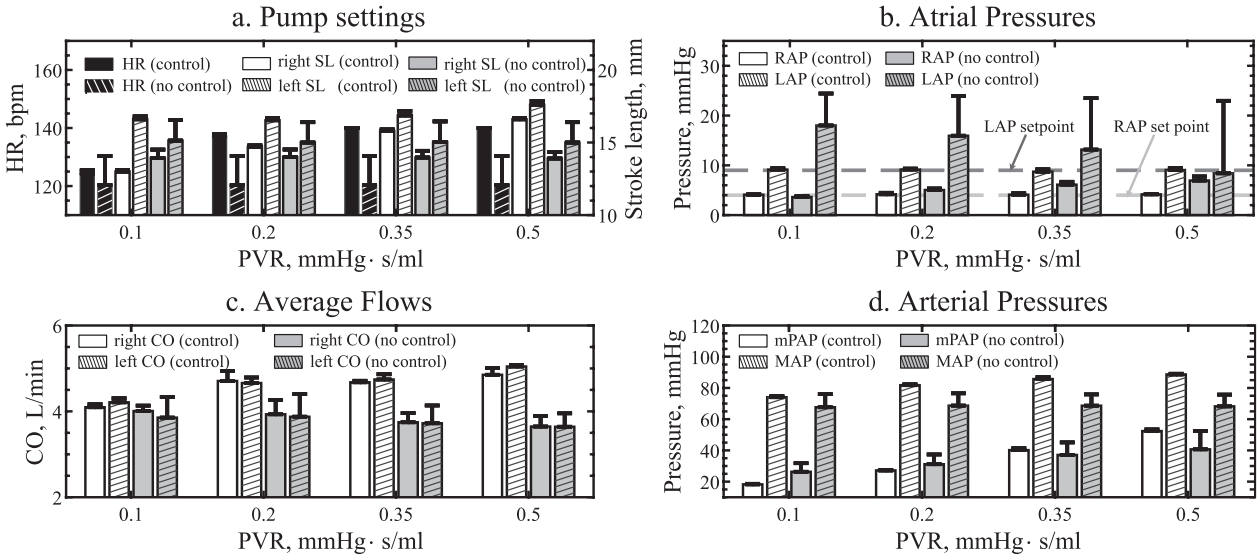

FIGURE 6 | (a) Heart rate and stroke length settings of the Realheart TAH operated with (control) and without (no control) at various PVR levels, corresponding to different stages of PH. The physiological controller helps keep (b) atrial pressures at their set points and improves (c) flow balance, in contrast to the uncontrolled case. (d) Arterial pressures are elevated under physiological control due to increased flows required to maintain pressures below set points at higher afterloads.

at rest to 140.0 ± 0.0 bpm in normal conditions, reaching 155.0 ± 0.0 bpm in severe PH. The controller stabilizes atrial pressures, mitigating fluctuations during exercise transitions. Without control, RAPs rise significantly, and MAP drops from resting levels.

3.4 | TAH Response to Simulated Sleep Condition

Figure 8 shows Realheart TAH performance during simulated sleep. With control on, CO decreases by 25% from rest, compared to 5% without control. HR drops by 12 bpm from rest across all PH levels. Atrial pressures remain within 2.5 mmHg of baseline with control, while uncontrolled settings show slight decreases. mPAP stabilizes with control in moderate/severe PH but remains unchanged without control. MAP increases by 20 mmHg during sleep across PH levels.

3.5 | Physiological Control Parameters

Figure 9 summarizes the physiological controller's performance across sleep, rest, exercise, and PH conditions. HR and SL increase from sleep to exercise, with SL exhibiting the largest relative change (80% right, 67% left). The left CO peaks during exercise and decreases during sleep. Without control, the left CO decreases with increasing PH severity, while RAPs rise significantly, and LAPs remain high (> 15 mmHg).

4 | Discussion

In this study, we conducted an in vitro evaluation of the adaptability of the Realheart physiological controller to physiologically respond to sleep and exercise in virtual patients with varying levels of PH. The tests were carried out using a HMCL.

4.1 | Left/Right Flow Balance

Maintaining a balance between left and right flow is crucial for TAHs. While passive self-regulating mechanisms [34] can manage flow in cardiac assist devices, an automatic physiological controller is needed when circulatory disruptions exceed self-adaptation capabilities, such as with high PVR [35].

Realheart's physiological controller regulates the left and right pumping units independently by adjusting HR and SL to maintain atrial pressures at predefined set points (set to 4 mmHg on the right and to 9 mmHg on the left in these experiments). Although flow balance is not an inherent property of the controller, it arises as a result of continuous pressure-based feedback. Flow imbalances, for instance arising from blood flow from the bronchial arteries emptying in the pulmonary venous system (broncho-arterial shunt), may lead to changes in atrial pressure, which in turn trigger compensatory adjustments in HR and SL to stabilize the atrial pressures at their setpoints.

Figure 6 illustrates this, comparing right and left CO with and without physiological control. Without control, CO is more variable, whereas with control, atrial pressures are stabilized and flow balance is achieved.

4.2 | Adaptation to PH

Under fixed pumping conditions, without physiological control, an increase in PVR leads to an elevated afterload on the right heart pump. This results in a reduced CO, which gradually decreases to below 4 L/min at high levels of PVR. In contrast, with physiological control, the CO at rest is maintained above 4 L/min and gradually increases as PVR rises. This behavior is due to the control strategy implemented by the physiological control system.

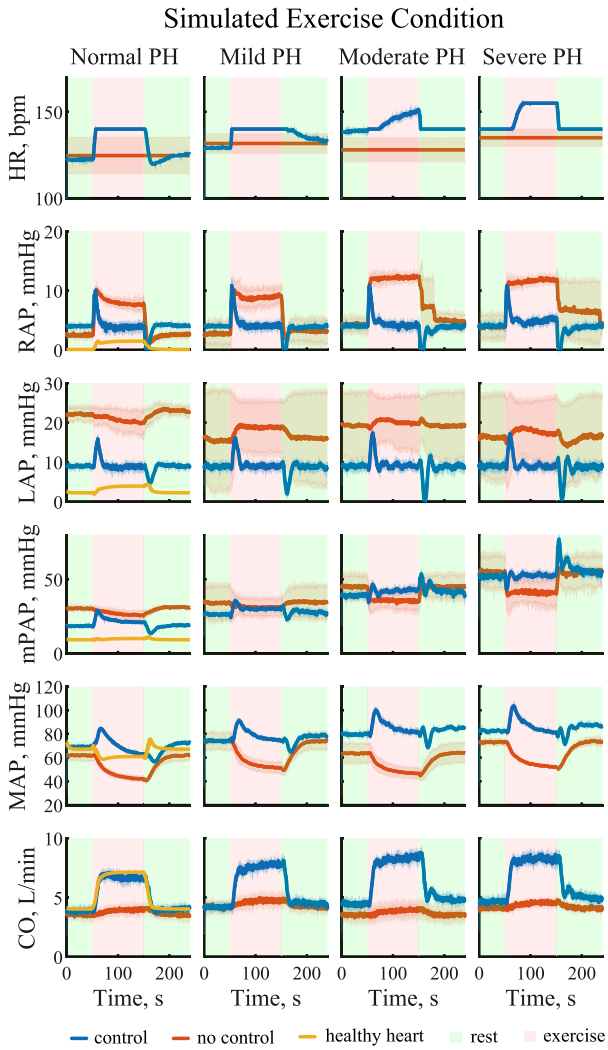

FIGURE 7 | Hemodynamic variables during simulated exercise, with (blue line) and without (red line) physiological control at various PH levels. Numerical results from the healthy heart computational model (yellow line) are included as reference. Solid lines denote mean values across repeats ($n = 3$), with shaded areas showing standard deviation. [Color figure can be viewed at wileyonlinelibrary.com] [Color figure can be viewed at wileyonlinelibrary.com]

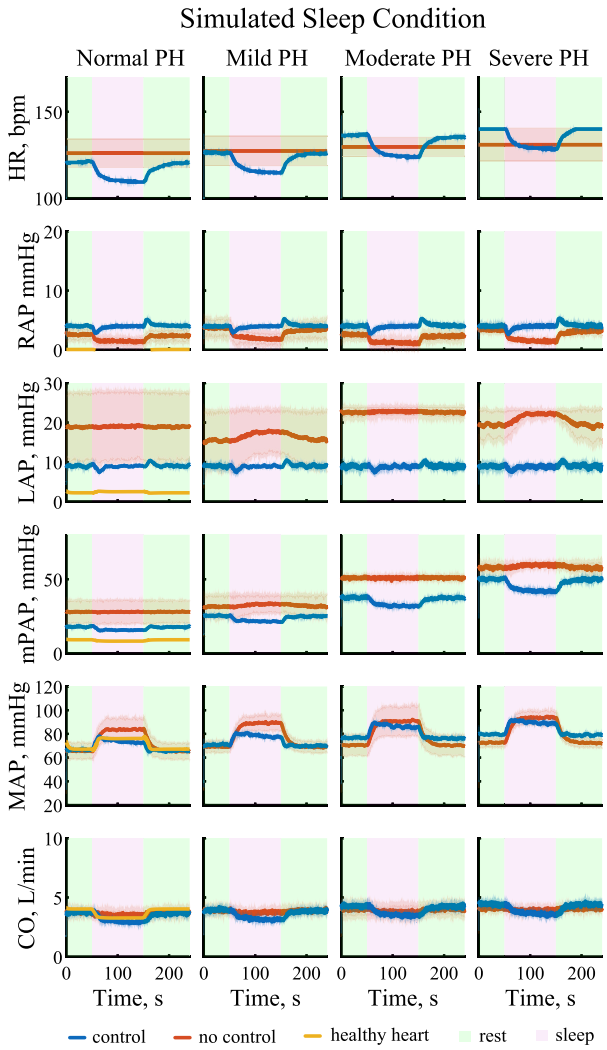

FIGURE 8 | Hemodynamic variables during simulated sleep, comparing with (blue line) and without (red line) physiological control at various PH levels. Reference numerical results from a healthy heart model (yellow line) are included. Solid lines denote mean values from experiments ($n = 3$); shaded regions show standard deviation. [Color figure can be viewed at wileyonlinelibrary.com] [Color figure can be viewed at wileyonlinelibrary.com]

High PVR reduces right ventricular outflow, causing fluid to accumulate in the right atrium. This leads to an increase in RAP while lowering LAP. In response, the physiological controller detects the elevated RAP and reacts by increasing the HR and the SL of the right ventricle. This raises CO and helps restore the atrial pressures to their set points. However, as PH worsens, the CO required to maintain these atrial pressures at rest also increases proportionally. Since PH was modeled via vasoconstriction in the pulmonary resistance arterioli, a blood volume shift to the systemic circulation might occur. This excess volume can elevate atrial pressures, activating the physiological controller to increase CO. As PH increases, more blood is redirected to the actively circulating blood volume, further raising atrial pressures and thus CO. This might explain why CO increases with rising PVR when physiological control is active.

4.3 | Heart Rate Adaptation

The physiological controller can adjust the HR across a broad spectrum (40–155 bpm) to respond to varying physiological conditions. As illustrated in Figure 7, HR peaks at 140 bpm during exercise in normal to mild PH cases, whereas, in moderate to severe PH, HR rises from 140 bpm at rest to 155 bpm during exercise. This is due to the physiological controller's operation limits, defined as HR $\leq$ 140 bpm for normal operation and 140 bpm $<$ HR $\leq$ 155 bpm for extreme conditions.

In fact, at higher PH levels and at rest conditions, the pump is close to the operational limit since it needs to cope with the high PVR. This situation is further aggravated by exercise, which causes a sudden increase in atrial pressures, mitigated by increasing the HR within the extreme mode range. On the other hand, during sleep, HR modulation happens well within safe

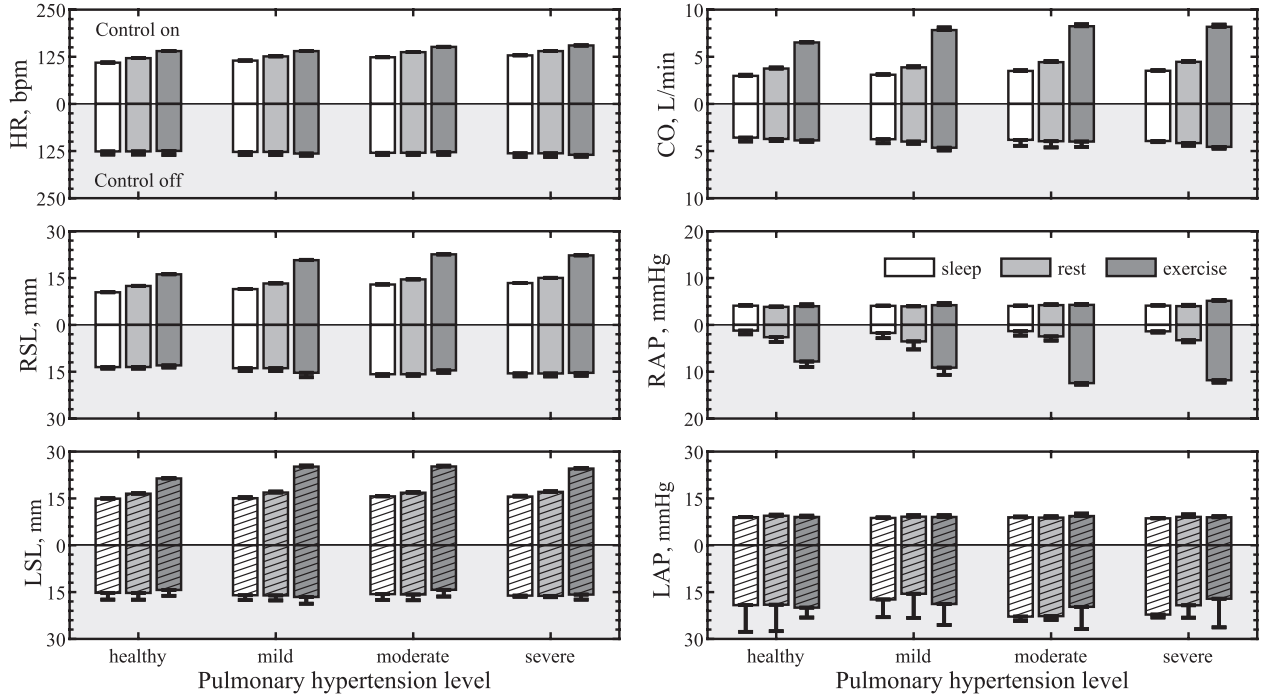

FIGURE 9 | Key pumping parameters, including heart rate (HR), right and left stroke lengths (RSL, LSL), left cardiac output (CO), and atrial pressures, were assessed across various physiological conditions and PH levels. Bar heights indicate the experimental mean, and error bars represent standard deviation. The positive y-axis (white background) indicates data with active physiological control, whereas the negative y-axis (gray background) shows data with the control disabled. With control, HR rises from sleep to exercise, significantly increasing left CO, while atrial pressures stay stable. Without control, left CO slightly increases from rest to exercise, but atrial pressures rise significantly, showing high variability.

limits because of the decreased metabolic demand, resulting in a slight reduction of CO at all PH levels.

4.4 | Pressure Control

Active control of the pumping parameter allows for rapid and stable adjustments of atrial pressures. Upon the onset of exercise, the atria experience a sudden pressure increase, which is attenuated and stabilized around the set points in approximately 20 s (Figure 7). This is crucial for flow regulation, as it shows that the pump can quickly adapt to changes in atrial pressure, which can be associated with changes in venous return, reflecting the varying metabolic demand of the body.

Although the pulmonary and aortic pressure response appeared to be modest during exercise, it remained relatively stable around the resting level. A similar response was observed in a study that evaluated TAH performance during exercise, and it is reported to be safe when exercise is carried out in a supervised setting [36]. However, not employing physiological control would result in a decreasing aortic pressure, which dropped by about 20 mmHg during exercise, demonstrating the importance of employing an active physiological control.

Pressure fluctuations appear to be less significant during sleep. However, physiological control is needed to regulate LAP, which can build up due to flow imbalance (Figure 8). Overall, physiological control manages atrial pressures across different physiological states, regardless of the PH level.

4.5 | Limitations

The physiological control system exhibited significant atrial pressure changes during rapid transition between physiological states. These fluctuations were minimal during sleep but more pronounced with exercise.

Positive atrial pressure fluctuations are usually manageable and can normalize within seconds. Negative fluctuations, however, should be avoided since they can cause suction events, leading to vessel collapse and fluid blockage, often when exercise stops abruptly, as shown in Figure 7 under severe PH. More research is required to assess the pressure threshold for a suction event, as it differs with various TAH settings. For instance, one study found suction events could occur at pressures below −3 mmHg, lower than any pressure recorded in our study [37].

To address this, future controller refinements may include adaptive PI tuning and acceleration-based sensing to detect postural changes and activity states. Additionally, a dual-control strategy, which combines preload- and afterload-dependent mechanisms, is under consideration to enhance overall stability and safety across different clinical scenarios.

Pronounced undershoots, particularly during transitions between exercise and rest, could be due to the slower reactions of the physiological controller compared to simulated cardiovascular changes. In fact, the model used in this study might inaccurately capture circulatory responses across scenarios because of difficulties in estimating some cardiovascular parameters (e.g.,

UVV changes). Future work should aim at adjusting PI parameters to enable a more robust and quicker pump response to physiological changes.

Moreover, flow redistribution due to broncho-arterial shunting is not currently represented in the cardiovascular model. In healthy individuals, the magnitude of this shunt is typically small (ranging from 0% to 2.8% of left cardiac output) and is often negligible. However, in patients with pulmonary conditions such as bronchiectasis or tuberculosis, shunt flows can reach up to 20% [38]. In recipients of a TAH, reported shunt flows range from 0 to 1.4 L/min [39], suggesting that compensatory mechanisms may be required to manage such variability.

Furthermore, PH in our model is simulated solely through vasoconstriction of the pulmonary resistance arterioli and does not account for other physiological mechanisms such as vascular remodeling or altered compliance, which may significantly influence the hemodynamic response.

Future implementations of the cardiovascular model may incorporate patient-specific features, such as dynamic broncho-arterial shunt behavior and anonymized clinical hemodynamic datasets from patients with advanced heart failure or pulmonary hypertension, to enable more personalized and robust evaluation of controller performance.

5 | Conclusion

The response of the Realheart physiological controller during sleep, rest, and exercise conditions was evaluated in vitro using simulated patients with varying degrees of PH. The physiological controller demonstrated superior adaptation capabilities in these scenarios compared to when the pump was operated with fixed parameters. CO increased significantly during exercise and decreased slightly during sleep, compared to the limited adjustments in CO observed when the physiological controller was not used. Atrial pressures remained consistently stabilized around their predefined set points. While arterial pressures exhibited a modest response during exercise, they remained stable around resting levels and did not drop drastically, as occurred without the physiological controller. Future work will focus on optimizing the physiological controller to respond more effectively to rapid physiological changes while avoiding suction events. Additionally, improvements to the numerical model will be made to account for patients with different BSA and to compare the pump's performance with other current TAH technologies.

Author Contributions

Emanuele Perra concept/design, data collection, data analysis/interpretation, drafting article, critical revision of the article, approval of the article. Seraina Anne Dual concept/design, data interpretation, critical revision of the article, and approval of the article. Ina Laura Perkins, Thomas Finocchiaro, Daniel Jonasson, Shaikh Faisal Zaman, Michael Broomé, data interpretation, critical revision of the article, approval of the article. Nils Brynedal Ignell critical revision of the article, approval of the article.

Acknowledgments

The work was carried out within the strategic innovation programme 'Smarter Electronics Systems', a joint initiative by Vinnova, Formas and the Swedish Energy Agency (Energimyndigheten). We thank and acknowledge VINNOVA (2022-0084, 2024-00592), Digital Futures of KTH for their financial support. The authors thank Dr. Marianne Schmid Daners at ETH Zurich for her expertise in replicating the HMCL.

Conflicts of Interest

Ina Laura Perkins, Thomas Finocchiaro, Daniel Jonasson, and Shaikh Faisal Zaman are employees and/or shareholders of Scandinavian Real Heart AB. Nils Brynedal Ignell has been an employee as well as a shareholder of Scandinavian Real Heart AB.

References

1. Z. Zhu, F. R. Li, Y. Jia, et al., "Association of Lifestyle With Incidence of Heart Failure According to Metabolic and Genetic Risk Status: A Population-Based Prospective Study," *Circulation: Heart Failure* 15, no. 9 (2022): e009592, https://doi.org/10.1161/CIRCHEARTFAILURE.122.009592.

2. A. Norhammar, J. Bodegard, M. Vanderheyden, et al., "Prevalence, Outcomes and Costs of a Contemporary, Multinational Population With Heart Failure," *Heart* 109 (2023): heartjnl2022321702, https://doi.org/10.1136/heartjnl-2022-321702.

3. G. Savarese and L. H. Lund, "Global Public Health Burden of Heart Failure," *Cardiac Failure Review* 3 (2017): 7.

4. S. D. Nathan, J. A. Barbera, S. P. Gaine, et al., "Pulmonary Hypertension in Chronic Lung Disease and Hypoxia," *European Respiratory Journal* 53, no. 1 (2019): 1801914, https://doi.org/10.1183/13993003.01914-2018.

5. P. P. Chang, J. C. Longenecker, N. Y. Wang, et al., "Mild vs Severe Pulmonary Hypertension Before Heart Transplantation: Different Effects on Posttransplantation Pulmonary Hypertension and Mortality," *Journal of Heart and Lung Transplantation* 24, no. 8 (2005): 998–1007, https://doi.org/10.1016/j.healun.2004.07.013.

6. Y. Krishnamurthy, L. B. Cooper, D. Lu, et al., "Trends and Outcomes of Patients With Adult Congenital Heart Disease and Pulmonary Hypertension Listed for Orthotopic Heart Transplantation in the United States," *Journal of Heart and Lung Transplantation* 35, no. 5 (2016): 619–624, https://doi.org/10.1016/j.healun.2015.12.017.

7. G. Ochsner, M. J. Wilhelm, R. Amacher, et al., "In Vivo Evaluation of Physiologic Control Algorithms for Left Ventricular Assist Devices Based on Left Ventricular Volume or Pressure," *ASAIO Journal* 63, no. 5 (2017): 568–577, https://doi.org/10.1097/MAT.0000000000000533.

8. A. Petrou, J. Lee, S. Dual, G. Ochsner, M. Meboldt, and D. M. Schmid, "Standardized Comparison of Selected Physiological Controllers for Rotary Blood Pumps: In Vitro Study," *Artificial Organs* 42, no. 3 (2018): E29–E42, https://doi.org/10.1111/aor.12999.

9. M. Vollkron, H. Schima, L. Huber, R. Benkowski, G. Morello, and G. Wieselthaler, "Development of a Reliable Automatic Speed Control System for Rotary Blood Pumps," *Journal of Heart and Lung Transplantation* 24, no. 11 (2005): 1878–1885, https://doi.org/10.1016/j.healun.2005.02.004.

10. J. Keenan and J. Pal, "The Need for Speed: Modulating Left Ventricular Assist Device Flow in Response to Varying Physiological Conditions," *Heart* 108, no. 13 (2022): 996–997, https://doi.org/10.1136/heartjnl-2022-320836.

11. M. Stapor, A. Pilat, A. Gackowski, et al., "Echo-Guided Left Ventricular Assist Device Speed Optimisation for Exercise Maximisation," *Heart* 108, no. 13 (2022): 1055–1062, https://doi.org/10.1136/heartjnl-2021-320495.

12. B. Kirn, M. Diedrich, T. Schmitz-Rode, U. Steinseifer, and S. V. Jansen, "Detection of Physiological Control Inputs Preload and Afterload From Intrinsic Pump Parameters in Total Artificial Heart," *Artificial Organs* 47, no. 5 (2023): 817–827, https://doi.org/10.1111/aor.14481.

13. I. Netuka, Y. Pya, B. Poitier, et al., "First Clinical Experience With the Pressure Sensor–Based Autoregulation of Blood Flow in an Artificial Heart," *ASAIO Journal* 67, no. 10 (2021): 1100–1108, https://doi.org/10.1097/MAT.0000000000001485.

14. S. A. Dual, J. Cowger, E. Roche, and A. Nayak, "The Future of Durable Mechanical Circulatory Support: Emerging Technological Innovations and Considerations to Enable Evolution of the Field," *Journal of Cardiac Failure* 30, no. 4 (2024): 596–609, https://doi.org/10.1016/j.cardfail.2024.01.011.

15. J. R. Crosby, K. J. DeCook, P. L. Tran, et al., "Physiological Characterization of the SynCardia Total Artificial Heart in a Mock Circulation System," *ASAIO Journal* 61, no. 3 (2015): 274–281, https://doi.org/10.1097/MAT.0000000000000192.

16. D. G. Tang, K. B. Shah, M. L. Hess, and V. Kasirajan, "Implantation of the Syncardia Total Artificial Heart," *Journal of Visualized Experiments* 1, no. 89 (2014): 50377, https://doi.org/10.3791/50377.

17. J. H. Karimov, K. Fukamachi, and R. C. Starling, eds., *Mechanical Support for Heart Failure: Current Solutions and New Technologies* (Springer International Publishing, 2020), https://doi.org/10.1007/978-3-030-47809-4.

18. Z. Szabo, J. Holm, A. Najar, G. Hellers, I. L. Pieper, and A. H. Casimir, "Scandinavian Real Heart (SRH) 11 Implantation as Total Artificial Heart (TAH)-Experimental Update," *Journal of Clinical & Experimental Cardiology* 9, no. 3 (2018): 2, https://doi.org/10.4172/2155-9880.1000578.

19. J. Feher, "5.8–The Cardiac Function Curve," in *Quantitative Human Physiology*, ed. J. Feher (Boston: Academic Press, 2012), 486–494.

20. C. S. Kwan-Gett, M. J. Crosby, A. Schoenberg, S. C. Jacobsen, and W. J. Kolff, "Control Systems for Artificial Hearts," *ASAIO Journal* 14, no. 1 (1968): 284 290.

21. N. N. Puri, J. K. Li, S. Fich, and W. Welkowitz, "Control System for Circulatory Assist Devices: Determination of Suitable Control Variables," *Transactions - American Society for Artificial Internal Organs* 28 (1982): 127–132.

22. T. Kitamura, "Left Atrial Pressure Controller Design for an Artificial Heart," *IEEE Transactions on Biomedical Engineering* 37, no. 2 (1990): 164–169, https://doi.org/10.1109/10.46256.

23. G. Ochsner, R. Amacher, A. Amstutz, et al., "A Novel Interface for Hybrid Mock Circulations to Evaluate Ventricular Assist Devices," *IEEE Transactions on Biomedical Engineering* 60, no. 2 (2013): 507–516, https://doi.org/10.1109/TBME.2012.2230000.

24. A. Petrou, M. Granegger, M. Meboldt, and M. Schmid Daners, "A Versatile Hybrid Mock Circulation for Hydraulic Investigations of Active and Passive Cardiovascular Implants," *ASAIO Journal* 65, no. 5 (2019): 495–502, https://doi.org/10.1097/MAT.0000000000000851.

25. E. Perra, O. Kreis, and S. A. Dual, "Showcasing Capabilities of a Hybrid Mock Circulation Loop for Investigation of Aortic Coarctation," in *Functional Imaging and Modeling of the HeartKTH*, ed. O. Bernard, P. Clarysse, N. Duchateau, J. Ohayon, and M. Viallon (Springer Nature Switzerland, 2023), 505–514.

26. L. Fresiello, A. Najar, N. Brynedal Ignell, et al., "Hemodynamic Characterization of the Realheart Total Artificial Heart With a Hybrid Cardiovascular Simulator," *Artificial Organs* 46, no. 8 (2022): 1585–1596, https://doi.org/10.1111/aor.14223.

27. S. Boës, G. Ochsner, R. Amacher, A. Petrou, M. Meboldt, and M. Schmid Daners, "Control of the Fluid Viscosity in a Mock Circulation," *Artificial Organs* 42, no. 1 (2018): 68–77, https://doi.org/10.1111/aor.12948.

28. M. Broomé, E. Maksuti, A. Bjällmark, B. Frenckner, and B. Janerot-Sjöberg, "Closed-Loop Real-Time Simulation Model of Hemodynamics and Oxygen Transport in the Cardiovascular System," *Biomedical Engineering Online* 12, no. 1 (2013): 69, https://doi.org/10.1186/1475-925X-12-69.

29. N. Stergiopulos, J. J. Meister, and N. Westerhof, "Determinants of Stroke Volume and Systolic and Diastolic Aortic Pressure," *American Journal of Physiology. Heart and Circulatory Physiology* 270, no. 6 (1996): H2050–H2059, https://doi.org/10.1152/ajpheart.1996.270.6.H2050.

30. J. P. Mynard, M. R. Davidson, D. J. Penny, and J. J. Smolich, "A Simple, Versatile Valve Model for Use in Lumped Parameter and One-Dimensional Cardiovascular Models," *International Journal for Numerical Methods in Biomedical Engineering* 28, no. 6–7 (2012): 626–641, https://doi.org/10.1002/cnm.1466.

31. A. Chaouat, A. S. Bugnet, N. Kadaoui, et al., "Severe Pulmonary Hypertension and Chronic Obstructive Pulmonary Disease," *American Journal of Respiratory and Critical Care Medicine* 172, no. 2 (2005): 189–194, https://doi.org/10.1164/rccm.200401-006OC.

32. D. Chemla, V. Castelain, P. Herve, Y. Lecarpentier, and S. Brimioulle, "Haemodynamic Evaluation of Pulmonary Hypertension," *European Respiratory Journal* 20, no. 5 (2002): 1314–1331, https://doi.org/10.1183/09031936.02.00068002.

33. M. M. Hoeper, H. A. Ghofrani, E. Grünig, H. Klose, H. Olschewski, and S. Rosenkranz, "Pulmonary Hypertension," *Deutsches Ärzteblatt International* 114, no. 5 (2017): 73–84, https://doi.org/10.3238/arztebl.2017.0073.

34. K. Fukamachi, A. Shiose, A. Massiello, et al., "Preload Sensitivity in Cardiac Assist Devices," *Annals of Thoracic Surgery* 95, no. 1 (2013): 373–380, https://doi.org/10.1016/j.athoracsur.2012.07.077.

35. H. A. Khalil, D. T. Kerr, M. A. Franchek, et al., "Continuous Flow Total Artificial Heart: Modeling and Feedback Control in a Mock Circulatory System," *ASAIO Journal* 54, no. 3 (2008): 249–255, https://doi.org/10.1097/MAT.0b013e3181739b70.

36. H. S. Kohli, J. Canada, R. Arena, et al., "Exercise Blood Pressure Response During Assisted Circulatory Support: Comparison of the Total Artifical Heart With a Left Ventricular Assist Device During Rehabilitation," *Journal of Heart and Lung Transplantation* 30, no. 11 (2011): 1207–1213, https://doi.org/10.1016/j.healun.2011.07.001.

37. H. Fumoto, D. J. Horvath, S. Rao, et al., "In Vivo Acute Performance of the Cleveland Clinic Self-Regulating, Continuous-Flow Total Artificial Heart," *Journal of Heart and Lung Transplantation* 29, no. 1 (2010): 21–26, https://doi.org/10.1016/j.healun.2009.05.035.

38. L. Cudkowicz, M. Calabresi, R. G. Nims, and F. D. Gray, "The Simultaneous Estimation of Right and Left Ventricular Outputs Applied to a Study of the Bronchial Circulation in Patients With Chronic Lung Disease," *American Heart Journal* 58, no. 5 (1959): 743–749, https://doi.org/10.1016/0002-8703(59)90233-9.

39. S. Bhunia and R. Kung, "Indirect Bronchial Shunt Flow Measurements in AbioCor Implantable Replacement Heart Recipients," *ASAIO Journal* 50, no. 3 (2004): 211–214, https://doi.org/10.1097/01.MAT.0000124101.70517.BF.